

1 CONFIDENTIAL

2 FEMS Yeast Research

3

4 **Recombination-stable multimeric green fluorescent protein**

5 **for characterization of weak promoter outputs in**

6 *Saccharomyces cerevisiae*

7

8 Research article

9 Running title: Recombination-stable multimeric GFP

10

11 Authors:

12 Peter Rugbjerg<sup>1</sup> – petru@biosustain.dtu.dk

13 Christoph Knuf<sup>1</sup> – chrik@biosustain.dtu.dk

14 Jochen Förster<sup>1</sup> – jfor@biosustain.dtu.dk

15 Morten O. A. Sommer<sup>1\*</sup> - msom@bio.dtu.dk

16

17 1) Novo Nordisk Foundation Center for Biosustainability, Technical University of

18 Denmark

19 Kogle Allé 6, DK-2970 Hørsholm, Denmark

20

21 \* Corresponding author

22

## 22 **Abstract**

23 Green fluorescent proteins (GFPs) are widely used for visualization of proteins to  
24 track localization and expression dynamics. However, phenotypically important  
25 processes can operate at too low expression levels for routine detection, i.e. be  
26 overshadowed by autofluorescence noise. While GFP functions well in translational  
27 fusions, the use of tandem GFPs to amplify fluorescence signals is currently avoided  
28 in *Saccharomyces cerevisiae* and many other microorganisms due to the risk of loop-  
29 out by direct-repeat recombination. We increased GFP fluorescence by translationally  
30 fusing three different GFP variants, yeast-enhanced GFP, GFP+ and superfolder GFP  
31 to yield a sequence-diverged triple GFP molecule 3vGFP with 74-84 % internal repeat  
32 identity. Unlike a single GFP, the brightness of 3vGFP allowed characterization of a  
33 weak promoter in *S. cerevisiae*. Utilizing 3vGFP, we further engineered a less leaky  
34 Cu<sup>2+</sup>-inducible promoter based on *CUPI*. The basal expression level of the new  
35 promoter was approx. 61 % below the wild-type *CUPI* promoter, thus expanding the  
36 absolute range of Cu<sup>2+</sup>-based gene control. The stability of 3vGFP towards direct-  
37 repeat recombination was assayed in *S. cerevisiae* cultured for 25 generations under  
38 strong and slightly toxic expression after which only limited reduction in fluorescence  
39 was detectable. Such non-recombinogenic GFPs can help quantify intracellular  
40 responses operating a low copy number in recombination-prone organisms.

41

42 **Keywords:** signal amplification, synthetic biology, promoter engineering, protein  
43 multimerization

44

## 44 **Introduction**

45 Green fluorescent protein (GFP) is an invaluable tool for real-time visualization of  
46 intracellular proteins. Since the initial cloning, numerous improvements, variants and  
47 applications have been developed (Snapp 2009; Miyawaki 2011). GFP is particularly  
48 useful for quantification of intracellular events, localizations and populations at  
49 single-cell resolution. However, a minimal expression level is required such that the  
50 fluorescent output exceeds the cell autofluorescence and produces detectable signals.  
51 Still, biologically important processes occur through the interaction of a few  
52 molecules per cell, which is hard to quantify using existing fluorescent proteins and  
53 non-specialized experimental setups (Raj and van Oudenaarden 2009; Li and Xie  
54 2011; Gahlmann and Moerner 2014). Further, the engineering of synthetic cell  
55 functionalities can depend on fine characterization and balancing of low gene  
56 expression levels (Ajikumar et al. 2010; Harton et al. 2013).

57 The strategies for improving fluorescent output signals include the design of new GFP  
58 variants such as GFP+, yeast-enhanced GFP (yEGFP) and superfolder GFP (sfGFP)  
59 (Cormack et al. 1997; Scholz et al. 2000; Pédelacq et al. 2006). Still, monitoring of  
60 single-molecule events such as chromosome movements in *Escherichia coli* has e.g.  
61 required multimerization of 96 DNA binding sites to localize enough fluorescent  
62 protein to produce a distinguishable signal (Xie et al. 2008). Artificial tethering of a  
63 bright yellow fluorescent protein (Venus YFP) to the inside *E. coli* cell membrane  
64 allowed a microscope-detectable signal from a single YFP-tagged protein (Yu et al.  
65 2006). Thus without techniques for single-molecule GFP sensitivity, the full-genome  
66 mapping of subcellular protein localization in *Saccharomyces cerevisiae* (yeastGFP)  
67 did not produce signals above background for 361 open reading frames (8 pct. of

68 total) otherwise shown to be expressed in the growth phase assayed (Ghaemmaghani  
69 et al. 2003; Huh et al. 2003). Equivalently, the issue of not detecting all low-  
70 expressing *S. cerevisiae* proteins was also observed when the GFP library was applied  
71 to flow cytometry (Newman et al. 2006).

72 In some contexts, simple overexpression may shed light over the lacking information,  
73 but since the location of many proteins is a result of interactions with other cell  
74 components, a radical change in copy number could easily result in artificial  
75 observations. In other situations, the target output is the activity of specific weak  
76 promoters, e.g. in synthetic biological circuits, fluorescence-coupled biosensors or  
77 when developing promoter libraries. Several technologies permit the engineering of  
78 new promoters, e.g. responsive to other inducer molecules by hybridizing with  
79 upstream TF-binding sites (Blazek and Alper 2013) or tuned to match fine, desirable  
80 transcription levels through mutagenesis of a strong native promoter (Nevoigt et al.  
81 2006). Difficulties in GFP detection may have been a limitation in these  
82 developments for weaker promoter levels, though low expression may be  
83 phenotypically important for a wide range of synthetic biology purposes. In synthetic  
84 circuit designs, any concealed information on the shape of dose-response curves  
85 inhibits the analysis of mechanistic clues otherwise given by the response curvature  
86 (Ang et al. 2013). In applications of metabolite biosensors, background-covered  
87 signal levels means that the full regulatory capability cannot be utilized, e.g. limiting  
88 subsequent fluorescence-activated cell sorting (FACS). Ultimately, such  
89 autofluorescence could conceal properly functional GFP completely (Billinton and  
90 Knight 2001).

91

92 The efforts aimed at reducing the autofluorescence target two phenomena: Simple  
93 medium autofluorescence arises from measuring fluorescence without isolating cells  
94 from medium, e.g. in continuously growing cultures. These effects can be reduced by  
95 the choice of medium or spectral unmixing by correcting for autofluorescence from a  
96 wavelength representing effects of the culture medium (Lichten et al. 2014).

97 However, the cell autofluorescence is a more central issue, i.a. resulting from the  
98 fluorescence of flavins and NAD(P)H (Billinton and Knight 2001). Cellular  
99 autofluorescence also impacts techniques such as flow cytometry and microscopy and  
100 the weak signal intensity must be amplified intrinsically to the cell.

101

102 Previous studies in mammalian cell lines have tackled the obstacle of cell  
103 autofluorescence using directly repeated GFPs typically fused three to six times in  
104 tandem using a small translational linker (Genové et al. 2005). By such approaches, it  
105 has been possible to achieve good linear increments in fluorescence signals. However,  
106 tandem repeats are problematic in organisms with proficient homologous  
107 recombination such as *Escherichia coli* or *S. cerevisiae* where recombination between  
108 DNA can happen within windows of identity at around 25 nucleotides (Ahn et al.  
109 1988). This could explain why tandem GFP methods are avoided in these organisms.  
110 However, even slight sequence divergence between repeats substantially decreases the  
111 rate of recombination as seen in the case of recombination between 350 bp inverted  
112 repeats, which was 4,600-fold reduced when sequence identity was reduced from 100  
113 % to 74 % in *S. cerevisiae* (Datta et al. 1997). Similar effects occur in *E. coli* where  
114 up to 1,000-fold reduction was observed following a reduction in repeat identity to 80  
115 % (Rayssiguier et al. 1989).

116 Thus, in this study we present a simple methodology to take advantage of the ability  
117 to add sequence divergence to tandem proteins while maintaining function through  
118 variation in amino acid sequence as well as synonymous codon usage. By fusing three  
119 different GFP variants that vary mainly at nucleotide-level, we produce a new triple  
120 tandem GFP (3vGFP) stabilized towards direct-repeat recombination. We  
121 demonstrate the utility of 3vGFP through a genetically triggered promoter (ON/OFF)  
122 and developing and characterizing a new version of a Cu<sup>2+</sup>-responsive promoter with  
123 reduced leakiness. Application of 3vGFP allowed visualization of weak signals that  
124 could not be separated from autofluorescence levels using the brightest individual  
125 GFP variant, superfolder GFP. Lastly, we test the stability towards recombination  
126 after culturing of the strain harboring 3vGFP through 25 generations.

## 127 **Materials and methods**

### 128 **Materials**

129 Unless otherwise stated, reagents were purchased from Sigma-Aldrich. Synthetic  
130 complete (SC) medium was prepared from 1.4 g/L synthetic complete drop-out mix  
131 lacking uracil, tryptophan, leucine and histidine (Y2001), 6.7 g/L yeast nitrogen base  
132 without amino acids (Y0626) and 20 g/L D-glucose, pH standardized to 5.6. When SC  
133 was supplemented with additional amino acids, 60 mg/L leucine, 20 mg/L uracil,  
134 20 mg/L histidine-HCl and 20 mg/L tryptophan was added. Yeast Peptone Dextrose  
135 medium contained 20 g/L D-glucose.

136 Oligonucleotides were purchased from Integrated DNA Technologies.

### 137 **Plasmids**

138 The plasmids employed in this study are listed in Table 1.

139 **Strains**

140 The strains analyzed in this study are listed in Table 2.

141 The following background strains were used to construct the strains:

142 *Saccharomyces cerevisiae* MaV203 (MAT $\alpha$ , *leu2-3,112*, *trp1-901*, *his3 $\Delta$ 200*, *ade2-*

143 *101*, *gal4 $\Delta$* , *gal80 $\Delta$* , *SPAL10::URA3*, *GAL1::lacZ*, *HIS3UAS GAL1::HIS3@LYS2*,

144 *can1<sup>R</sup>*, *cyh2<sup>R</sup>*) (Purchased from Life Technologies).

145 *Saccharomyces cerevisiae* PRa18 (MAT $\alpha$ , *leu2-3,112*, *trp1-901*, *his3 $\Delta$ 200*, *ade2-101*,

146 *gal4 $\Delta$* , *gal80 $\Delta$* , *GAL1::lacZ*, *can1<sup>R</sup>*, *cyh2<sup>R</sup>*) Derived from *S. cerevisiae* MaV203.

147 *Saccharomyces cerevisiae* PRa26: MAT $\alpha$ , *leu2-3,112*, *trp1-901*, *his3 $\Delta$ 200*, *ade2-101*,

148 *gal4 $\Delta$* , *gal80 $\Delta$* , *GAL1::lacZ*, *rad16::KanMX*, *can1<sup>R</sup>*, *cyh2<sup>R</sup>*. Derived from *S. cerevisiae*

149 PRa18.

150 *Saccharomyces cerevisiae* CfB1010 (MAT $\alpha$ ; *ura3-52*; *his3 $\Delta$ 1*; *leu2-3/112*; *MAL2-8<sup>c</sup>*;

151 *SUC2*; *are2 $\Delta$ ::loxP-KanMX*; *X-3::tHMG1-P<sub>TEFI</sub>-P<sub>PGK1</sub>-AtATR2*). Derived from *S.*

152 *cerevisiae* CEN.PK 102-5B.

### 153 **Construction of 3vGFP plasmids**

154 Plasmids were constructed by uracil-excision (USER) cloning. The general method  
155 for USER cloning was based on agarose gel-purification of the PCR products  
156 amplified using DNA polymerase X7 (Nørholm 2010). These were mixed in an  
157 equimolar 20  $\mu$ L reaction with 0.5  $\mu$ L USER enzyme (New England Biolabs) and 0.5  
158  $\mu$ L DpnI FastDigest (Thermo Scientific) in FastDigest buffer at 37 degrees C for 1-2  
159 hours. Following 25 minutes at room temperature, 2.5  $\mu$ L reaction was transformed  
160 into *E. coli*. Correctly cloned plasmids were identified using restriction analysis and  
161 DNA sequencing. The detailed use of oligonucleotides for assembly of all plasmids is  
162 described in Supplementary data.

### 163 **Construction of strains**

164 Plasmids and DNA for chromosomal targeting was introduced in *S. cerevisiae* by  
165 methods described previously (Gietz and Schiestl 2007). The PRa18 strain was  
166 constructed from the MaV203 strain by deletion of *SPAL10::URA3* through  
167 replacement with a *kanMX* gene deletion cassette flanked by loxP recombination sites  
168 from the pUG6 plasmid as described before (Güldener et al. 1996). DNA flanks to  
169 direct homologous recombination of the cassette to the chromosomal locus were  
170 generated by PCR on *S. cerevisiae* MaV203 gDNA spanning a fragment from 5'-  
171 CCATTCAACTAACATCACAC to 5'-CCTTCACCATAAATATGCC (upstream  
172 flank) and from 5'-CTCACAAATTAGAGCTTC to 5'-CCCATATCCAACCTCCAA  
173 (downstream flank). These flanks were cloned to the *kanMX* gene deletion cassette  
174 and transformed into yeast. The *kanMX* cassette was looped out by heterologous  
175 expression of Cre recombinase from the pSH47 plasmid (Güldener et al. 1996). To  
176 construct PRa26 subsequently, the chromosomal *HIS3* gene within the *rad16* locus



177 was deleted using the same *kanMX* approach. The targeting flanks spanned regions  
178 from 5'- AGTTGGTACACCAGTTATACGG to 5'-  
179 AAAGCATAGGATACCGAGAAAC (upstream flank) and 5'-  
180 TGACATCACCCGAAAAGAAGC to 5'- GATTATGGTTACGATGTCGA  
181 (downstream flank).

182 To construct PRa114, the pTEF1-3vGFP construct was chromosomally integrated into  
183 the PRa18 strain using divisible selection (Rugbjerg et al. 2015). DNA fragments for  
184 integration was liberated from the vector pDS1U-X2-3vGFP by digestion with *SmiI*  
185 and transformed into yeast along with empty divisible selection plasmids pDS2 and  
186 pDS3 in order to reconstitute the selectable Ura<sup>+</sup> phenotype.

187 To construct respectively CK24 and CK28 from the Cfb1010 strain, the pCUP1-  
188 3vGFP and pCUP1dim-3vGFP was chromosomally integrated by cloning into the  
189 EasyClone integrative vectors (Jensen et al. 2013). The DNA fragments for  
190 integration were obtained through *NotI* digestion of the vectors pCfb258-CUP1-  
191 3vGFP and pCfb258-CUP1-SPO13-3vGFP respectively, followed by agarose gel  
192 purification.

### 193 **Estimation of TEF1-3vGFP fitness cost**

194 Microtiter cultures of 200  $\mu$ L YPD was inoculated by 100x backdilution of overnight  
195 YPD pre-cultures of PRa114 and PRa108, each inoculated from single colonies. The  
196 cultures were cultivated in a 96-well plate at 30 deg. C and continuous shaking in an  
197 ELx808 plate reader (BioTek), set to measure optical density every 15 minutes at  
198 OD<sub>630</sub>. The plate was covered with a BreathSeal (Greiner Bio-one) and plastic lid.  
199 Growth rates were calculated for all three biological replicates by exponential  
200 regression between OD<sub>630</sub> and time (hours) during the same OD<sub>630</sub> span of

201 exponential growth phase. All OD<sub>630</sub> values were initially standardized to the time  
202 zero reading to account for differences in seal absorbance.

### 203 **Cultivations for stability tests**

204 The PRa114 strain was cultured from a single colony inoculated in 25 mL YPD  
205 medium and cultured at 30 deg. C and 250 rpm horizontal shaking in three parallel  
206 lineages. By measuring OD<sub>600</sub>, the number of generations passed was calculated. 2 %  
207 of the culture was passed to fresh medium and grown again until totally 25  
208 generations had passed. For comparison between cultured population and reference  
209 strain, approx. 25 µL of each cell population was inoculated in YPD medium at the  
210 same time and cultured at 30 deg. C for 16 hours with 250 rpm horizontal shaking.

### 211 **Fluorescence measurements**

212 Pre-cultures in selective SC medium were inoculated from single colonies and  
213 cultures overnight at 30 deg. C. From these, 200 µL microtiter cultures of selective  
214 SC medium were inoculated and cultured at 30 deg. C with 300 rpm horizontal  
215 shaking in an Innova shaking incubator for 16 hours. As cover, the microtiter plates  
216 were covered with a BreathSeal (Greiner Bio-one) and a plastic lid.  
217 The cell cultures were diluted approx. 1:100 in FACS flow buffer (BD Biosciences)  
218 and analyzed on a LSR Fortessa flow cytometer (BD Biosciences) equipped with a  
219 blue laser (488 nm) and set to measure 10,000 cells within a gate defined by forward  
220 and side scatter to capture all yeast cells. A FITC filter (530/30 nm) was used to  
221 measure GFP fluorescence reporting the area of the measured peaks. The laser voltage  
222 was adjusted to optimally utilize the dynamic range of detection. Data was processed

223 and visualized as histograms with FlowJo version 10 (default settings) by overlaying  
224 the populations for each particular comparison.

225

## 226 **Sequence alignment**

227 Simple nucleotide and protein sequence alignment was performed using the ClustalO  
228 algorithm (Sievers et al. 2011).

229

## 229 **Results and discussion**

### 230 **Amplification of fluorescence by tandems of differently encoded GFPs**

231 To amplify the fluorescence signal of a GFP molecule while keeping transcription  
232 strength constant, the new 3vGFP protein was engineered by fusion of nucleotide  
233 sequences encoding yEGFP, GFP<sup>+</sup> and sfGFP (Cormack et al. 1997; Pédelacq et al.  
234 2006) (Fig. 1A). Two glycine residues were introduced as translational linker in each  
235 junction. The fluorescence of 3vGFP was evaluated when expressed from a weak *S.*  
236 *cerevisiae* hybrid promoter (p*SPAL10*) (Vidal et al. 1996) based on p*SPO13* to mimic  
237 low-expression applications (Huang and Schreiber 1997; Harton et al. 2013). The  
238 low-level strength of p*SPAL10* is attained by utilizing the UME6 repressor binding  
239 site naturally present within the *SPO13* promoter, which allows very low expression  
240 levels e.g. useful for control of cell growth. Further, GAL4-binding sites fused 238 bp  
241 upstream of start codon provide an upstream activating sequence, allowing  
242 transcription factor-based ON/OFF inputs.

243 The output fluorescence was first evaluated with single sfGFP (Fig. 1B), which is the  
244 individually brightest of the three GFPs tested. However, the fluorescence levels  
245 could not be distinguished from the control strain devoid of genes encoding GFP  
246 (PRa108). In contrast, the fluorescence of a strain (PRa106) carrying the gene  
247 encoding 3vGFP controlled by the same promoter was 3-fold higher than the  
248 background level and thus the level of the single sfGFP strain (Fig. 1B).

249

250 To test the utility of 3vGFP as output signal in a synthetic biology setting, we  
251 constructed versions of the strain with the p*SPAL10* promoter turned OFF. The

252 promoter is activated (ON) when a hybrid GAL4 activation domain binds a cognate  
253 hybrid GAL4 DNA-binding domain, which interacts with GAL4-binding sites of  
254 pSPAL10. The protein-protein interaction domains were based on the known Krev1  
255 and RalGDS interaction domains (Herrmann et al. 1996). However omitting the  
256 DNA-binding domain prevents reconstitution of a functional transactivator (OFF).  
257 These ON/OFF effects of present DNA-binding domain remained hidden below the  
258 background levels of the sfGFP strains, while observable in strains with 3vGFP as  
259 output (Fig. 1B).

260

261 **Figure 1**

## 262 **Stability towards recombination**

263 Direct-repeat recombination in mitotic *S. cerevisiae* is reported to occur at rates  
264 between  $5.8 \cdot 10^{-5}$  and  $12 \cdot 10^{-5}$  per cell generation for repeats of several kilo base pair  
265 identity (Dornfeld and Livingston 1992). This recombination rate is linearly  
266 dependent on identity length at such long segments, however the rate drops rapidly  
267 below the minimal efficient processing segment (MEPS) length at around 250 bp in *S.*  
268 *cerevisiae* (Jinks-Robertson et al. 1993). While internal identity of 3vGFP ranges 74-  
269 84 % (Fig. 2B), the identical segments are maximally at a ten-fold shorter length than  
270 the MEPS.

271 To test the recombination stability of 3vGFP, we wanted to measure whether the  
272 fluorescence levels originating from 3vGFP would attenuate following repeated  
273 culturing. While the 3vGFP molecule is engineered to limit direct-repeat  
274 recombination, long-term cultivation could potentially still lead to this especially if  
275 favored by a concurrent fitness advantage. To test stability at high expression level,  
276 we therefore also chromosomally integrated *3vGFP* under control of the strong

277 promoter from *TEF1* i.e. at a level surpassing the intended use of 3vGFP. Expressing  
278 3vGFP from the *TEF1* promoter caused a considerable cost in fitness of approx. 15 %  
279 in YPD, reducing the growth rate from an average of 0.35 hr<sup>-1</sup> to 0.30 hr<sup>-1</sup> compared  
280 to the negative control strain PRa108. Following culturing by serial passing (2 %) of  
281 liquid cultures for 25 generations of three parallel lineages, single-cell level analysis  
282 revealed that the average fluorescence level of the cell population had diminished by  
283 7 percent, perhaps due to spontaneous direct-repeat recombination. The single cell-  
284 level visualization indicated a slight left-shift of the population (Fig 2). These results  
285 exemplify that direct-repeat recombination can occur within 3vGFP in *S. cerevisiae*  
286 and if selected for, these effects can become significant. However, since 3vGFP is  
287 intended for use at levels of low expression, a fitness advantage is not likely to further  
288 drive diminished fluorescence at a typical utility of 3vGFP.

289

290 **Figure 2.**

291

291 **Application of 3vGFP to construct an inducible promoter with reduced leakiness**

292 Inducible promoters are important for development of e.g. synthetic genetic circuits,  
293 but the leakiness levels can be problematic in certain uses. To demonstrate the utility  
294 of 3vGFP, we therefore wanted to use it as output for genetic re-engineering of the  
295 popular  $\text{Cu}^{2+}$ -responsive promoter of *S. cerevisiae* *CUPI*. *pCUI* has been employed  
296 in many different biotechnological cases (Labbé and Thiele 1999; Scholz et al. 2000;  
297 Rugbjerg et al. 2013), but displays considerable baseline activity (leakiness). *pCUI*  
298 induction results from elevated  $\text{Cu}^{2+}$  concentrations mediated through binding of  $\text{Cu}^{2+}$   
299 to the ACE1 transcription factor, which in turn binds to upstream activating sequence  
300 (UAS) elements of *pCUI* (Huibregtse 1989; Evans et al. 1990) (elements  
301 schematically depicted in Fig. 3A). The leakiness level of *pCUI* measured with  
302 3vGFP corresponded to 2.5-fold the cell autofluorescence (Fig. 3B). Based on the  
303 regulatory mechanism of ACE1, we anticipated that trace levels of  $\text{Cu}^{2+}$  in the growth  
304 medium did not cause this leakiness, but rather assumed this basal transcriptional  
305 activity to be ACE1-independent. Accordingly, as strategy we hypothesized that  
306 swapping the promoter region downstream of ACE1 UASs for a transcriptionally  
307 repressed promoter could provide attenuation, while maintaining the response to  
308 ACE1-dependent induction. We therefore combined the upstream region of *pCUI* (-  
309 149 to -454) containing three ACE1-binding sites, with part of the *S. cerevisiae*  
310 *pSPO13* (-1 to -157) including its UME6 repressor-binding site (Fig. 3A). This new  
311 promoter (*pCUI<sub>dim</sub>*) controlling 3vGFP resulted in fluorescence that was reduced  
312 approx. 61 % (before background-subtraction) to levels close to the cell  
313 autofluorescence (Fig. 3B), while the promoter remained responsive to addition of  
314  $\text{Cu}^{2+}$  (Fig. 3C).

315

316 **Figure 3**

317

318 The recombination-stabilized tandem GFP described in this study can enable  
319 characterization of minimally expressed genes in recombination-efficient organisms  
320 such as *S. cerevisiae* and other yeasts. As shown in this study, 3vGFP allowed  
321 characterization of the activation of a weak promoter and accordingly characterization  
322 of manipulations taking place at such low expression levels. Further, this particular  
323 approach of recombination-stabilizing GFPs with different protein and nucleotide  
324 sequences can be scaled in number. Recent brighter fluorescent proteins could be  
325 applied such as mNeonGreen (Shaner et al. 2013).

326 In principle, sequence divergence could be generated strictly at nucleotide level  
327 through codon optimization of segments encoding the same protein. Codon  
328 optimization can however introduce significant effects on the translation efficiencies  
329 (Goodman et al. 2013). Another concern may be spurious promoter/RBS activities,  
330 which could theoretically cause transcription and translation initiation from locations  
331 within the tandem GFP, thus producing truncated tandem proteins. Such situations  
332 would complicate the isolation of promoter responses and might require alleviation of  
333 the second and third GFP start codon.

334 An alternative method for assessment of promoter activities could be the use of the  
335 fluorescent RNA of the Spinach family, which bypasses the step of translation since  
336 the RNA forms the fluorescent signal (Paige et al. 2012; Pothoulakis et al. 2014).

337 However, while the technology has potential for synthetic biological use, its general  
338 applicability remains to be seen, such as the detection limits for low expression levels.

339 Further relevant, fluorescent *in situ* hybridization for RNA (RNA FISH) is a



340 technique allowing sensitive detection of transcripts at single-cell level (Zenklusen et  
341 al. 2008). This alleviates genetic engineering, but entails more sample treatment than  
342 for detection of GFP fluorescence.

343 In this study, a new simple strategy for engineering tandem fluorescent proteins was  
344 employed to produce brighter GFP signals with improved stability towards loop-out  
345 recombination. GFPs with sequence variation mainly at nucleotide level were  
346 translationally linked to form a recombination-stabilized tandem GFP molecule  
347 3vGFP. Such GFPs could be useful for characterizing promoter activities in the range  
348 where normal single GFP signals fall below the cell autofluorescence levels. We  
349 specifically applied the 3vGFP molecule to characterize the ON/OFF levels of a weak  
350 promoter, which was not possible using a single sfGFP, and to develop a new hybrid  
351  $\text{Cu}^{2+}$ -responsive promoter pCUP1dim with lower leakiness level. The plasmid pCU2-  
352 3vGFP encompassing the nucleotide sequence of 3vGFP and pCUP1dim will be  
353 deposited at the Addgene repository.

## 354 **Competing interests**

355 The authors declare that they have no competing interests.

## 356 **Funding**

357 This work was supported by the Novo Nordisk Foundation, the European Union  
358 Seventh Framework Programme (FP7-KBBE-2013-7-single-stage) under Grant  
359 agreement no. 613745, Promys, and Deutsche Bundesstiftung Umwelt,.

## 360 **Acknowledgement**

361 George Church is acknowledged for sfGFP encoded on pJ251-GERC (AddGene  
362 plasmid 47441).  
363

## 363 References

- 364 Ahn BY, Dornfeld KJ, Fagrelus TJ, Livingston DM. 1988. Effect of limited homology on gene  
365 conversion in a *Saccharomyces cerevisiae* plasmid recombination system. *Mol. Cell. Biol.*  
366 8:2442–2448.
- 367 Ajikumar PK, Xiao W-H, Tyo KEJ, Wang Y, Simeon F, Leonard E, Mucha O, Phon TH, Pfeifer B,  
368 Stephanopoulos G. 2010. Isoprenoid pathway optimization for Taxol precursor overproduction in  
369 *Escherichia coli*. *Science* 330:70–74.
- 370 Ang J, Harris E, Hussey B. 2013. Tuning Response Curves for Synthetic Biology. *ACS Synth. Biol.*  
371 [Internet]:547–567. Available from: <http://pubs.acs.org/doi/abs/10.1021/sb4000564>
- 372 Billinton N, Knight a W. 2001. Seeing the wood through the trees: a review of techniques for  
373 distinguishing green fluorescent protein from endogenous autofluorescence. *Anal. Biochem.*  
374 [Internet] 291:175–197. Available from: <http://www.ncbi.nlm.nih.gov/pubmed/11401292>
- 375 Blazeck J, Alper HS. 2013. Promoter engineering: Recent advances in controlling transcription at the  
376 most fundamental level. *Biotechnol. J.* 8:46–58.
- 377 Cormack B, Bertram G, Egerton M. 1997. Yeast-enhanced green fluorescent protein (yEGFP): a  
378 reporter of gene expression in *Candida albicans*. *Microbiology* [Internet] 143:303–311. Available  
379 from: <http://mic.sgmjournals.org/content/143/2/303.short>
- 380 Datta A, Hendrix M, Lipsitch M, Jinks-Robertson S. 1997. Dual roles for DNA sequence identity and  
381 the mismatch repair system in the regulation of mitotic crossing-over in yeast. *Proc. Natl. Acad.*  
382 *Sci.* [Internet] 94:9757–9762. Available from: <http://www.pnas.org/content/94/18/9757.short>
- 383 Dornfeld KJ, Livingston DM. 1992. Plasmid recombination in a *rad52* mutant of *Saccharomyces*  
384 *cerevisiae*. *Genetics* 131:261–276.
- 385 Evans C, Engelke D, Thiele D. 1990. ACE1 Transcription Factor Produced in *Escherichia coli* Binds  
386 Multiple Regions within Yeast Metallothionein Upstream Activation site Sequences. *Mol. Cell.*  
387 *Biol.* [Internet] 10:426–429. Available from: <http://mcb.asm.org/content/10/1/426.short>
- 388 Gahlmann A, Moerner WE. 2014. Exploring bacterial cell biology with single-molecule tracking and  
389 super-resolution imaging. *Nat. Rev. Microbiol.* [Internet] 12:9–22. Available from:  
390 <http://www.ncbi.nlm.nih.gov/pubmed/24336182>
- 391 Genové G, Glick B, Barth A. 2005. Brighter reporter genes from multimerized fluorescent proteins.  
392 *Biotechniques* [Internet] 39:814–822. Available from:  
393 <http://www.biotechniques.com/article/05396BM02>
- 394 Ghaemmaghami S, Huh W-K, Bower K, Howson RW, Belle A, Dephoure N, O’Shea EK, Weissman  
395 JS. 2003. Global analysis of protein expression in yeast. *Nature* [Internet] 425:737–741.  
396 Available from: <http://www.ncbi.nlm.nih.gov/pubmed/14562106>
- 397 Gietz RD, Schiestl RH. 2007. High-efficiency yeast transformation using the LiAc/SS carrier  
398 DNA/PEG method. *Nat. Protoc.* [Internet] 2:31–34. Available from:  
399 <http://www.ncbi.nlm.nih.gov/pubmed/17401334>
- 400 Goodman D, Church G, Kosuri S. 2013. Causes and effects of N-Terminal Codon Bias in Bacterial  
401 Genes. *Science* (80-. ). [Internet] 342:475–479. Available from:  
402 <http://www.sciencemag.org/content/342/6157/475.short>

- 403 Güldener U, Heck S, Fielder T, Beinhauer J, Hegemann JH. 1996. A new efficient gene disruption  
404 cassette for repeated use in budding yeast. *Nucleic Acids Res.* [Internet] 24:2519–2524.  
405 Available from:  
406 [http://www.pubmedcentral.nih.gov/articlerender.fcgi?artid=145975&tool=pmcentrez&rendertype](http://www.pubmedcentral.nih.gov/articlerender.fcgi?artid=145975&tool=pmcentrez&rendertype=abstract)  
407 [=abstract](http://www.pubmedcentral.nih.gov/articlerender.fcgi?artid=145975&tool=pmcentrez&rendertype=abstract)
- 408 Harton M, Wingler L, Cornish V. 2013. Transcriptional Regulation Improves the Throughput of Three-  
409 Hybrid Counter Selections in *Saccharomyces cerevisiae*. *Biotechnol. J.* [Internet]:1–23. Available  
410 from: <http://onlinelibrary.wiley.com/doi/10.1002/biot.201300186/abstract>
- 411 Herrmann C, Horn G, Spaargaren M, Wittinghofer A. 1996. Differential Interaction of the Ras Family  
412 GTP-binding Proteins H-Ras, Rap1A, and R-Ras with the Putative Effector Molecules Raf  
413 Kinase and Ral-Guanine Nucleotide Exchange Factor. *J. Biol. Chem.* [Internet] 271:6794–6800.  
414 Available from: <http://www.jbc.org/cgi/doi/10.1074/jbc.271.12.6794>
- 415 Huang J, Schreiber SL. 1997. A yeast genetic system for selecting small molecule inhibitors of protein-  
416 protein interactions in nanodroplets. *Proc. Natl. Acad. Sci. U. S. A.* [Internet] 94:13396–13401.  
417 Available from:  
418 [http://www.pubmedcentral.nih.gov/articlerender.fcgi?artid=28315&tool=pmcentrez&rendertype](http://www.pubmedcentral.nih.gov/articlerender.fcgi?artid=28315&tool=pmcentrez&rendertype=abstract)  
419 [=abstract](http://www.pubmedcentral.nih.gov/articlerender.fcgi?artid=28315&tool=pmcentrez&rendertype=abstract)
- 420 Huh W-K, Falvo J V, Gerke LC, Carroll AS, Howson RW, Weissman JS, O’Shea EK. 2003. Global  
421 analysis of protein localization in budding yeast. *Nature* [Internet] 425:686–691. Available from:  
422 <http://www.ncbi.nlm.nih.gov/pubmed/14562095>
- 423 Huibregtse J. 1989. Copper-induced binding of cellular factors to yeast metallothionein upstream  
424 activation sequences. *Proc. Natl. Acad. Sci.* [Internet] 86:65–69. Available from:  
425 <http://www.pnas.org/content/86/1/65.short>
- 426 Jensen NB, Strucko T, Kildegaard KR, David F, Maury J, Mortensen UH, Forster J, Nielsen J,  
427 Borodina I. 2013. EasyClone: method for iterative chromosomal integration of multiple genes in  
428 *Saccharomyces cerevisiae*. *FEMS Yeast Res.* [Internet]:1–11. Available from:  
429 <http://www.ncbi.nlm.nih.gov/pubmed/24151867>
- 430 Jinks-Robertson S, Michelitch M, Ramcharan S. 1993. Substrate length requirements for efficient  
431 mitotic recombination in *Saccharomyces cerevisiae*. *Mol. Cell. Biol.* 13:3937–3950.
- 432 Labbé S, Thiele D. 1999. Copper ion inducible and repressible promoter systems in yeast. *Methods*  
433 *Enzymol.* [Internet] 306:145–153. Available from:  
434 <http://www.sciencedirect.com/science/article/pii/S0076687999060103>
- 435 Li G-W, Xie XS. 2011. Central dogma at the single-molecule level in living cells. *Nature* [Internet]  
436 475:308–315. Available from:  
437 [http://www.pubmedcentral.nih.gov/articlerender.fcgi?artid=3600414&tool=pmcentrez&renderty](http://www.pubmedcentral.nih.gov/articlerender.fcgi?artid=3600414&tool=pmcentrez&rendertype=abstract)  
438 [pe=abstract](http://www.pubmedcentral.nih.gov/articlerender.fcgi?artid=3600414&tool=pmcentrez&rendertype=abstract)
- 439 Lichten C a, White R, Clark IBN, Swain PS. 2014. Unmixing of fluorescence spectra to resolve  
440 quantitative time-series measurements of gene expression in plate readers. *BMC Biotechnol.*  
441 [Internet] 14:11. Available from:  
442 [http://www.pubmedcentral.nih.gov/articlerender.fcgi?artid=3917901&tool=pmcentrez&renderty](http://www.pubmedcentral.nih.gov/articlerender.fcgi?artid=3917901&tool=pmcentrez&rendertype=abstract)  
443 [pe=abstract](http://www.pubmedcentral.nih.gov/articlerender.fcgi?artid=3917901&tool=pmcentrez&rendertype=abstract)
- 444 Miyawaki A. 2011. Proteins on the move: insights gained from fluorescent protein technologies. *Nat.*  
445 *Rev. Mol. Cell Biol.* [Internet] 12:656–668. Available from:  
446 <http://www.ncbi.nlm.nih.gov/pubmed/21941275>

- 447 Nevoigt E, Kohnke J, Fischer CR, Alper H, Stahl U, Stephanopoulos G. 2006. Engineering of promoter  
448 replacement cassettes for fine-tuning of gene expression in *Saccharomyces cerevisiae*. *Appl.*  
449 *Environ. Microbiol.* 72:5266–5273.
- 450 Newman JRS, Ghaemmaghami S, Ihmels J, Breslow DK, Noble M, DeRisi JL, Weissman JS. 2006.  
451 Single-cell proteomic analysis of *S. cerevisiae* reveals the architecture of biological noise. *Nature*  
452 441:840–846.
- 453 Nørholm MHH. 2010. A mutant Pfu DNA polymerase designed for advanced uracil-excision DNA  
454 engineering. *BMC Biotechnol.* [Internet] 10:21. Available from:  
455 <http://www.pubmedcentral.nih.gov/articlerender.fcgi?artid=2847956&tool=pmcentrez&rendertype=abstract>  
456
- 457 Paige JS, Nguyen-Duc T, Song W, Jaffrey SR. 2012. Fluorescence imaging of cellular metabolites with  
458 RNA. *Science* [Internet] 335:1194. Available from:  
459 <http://www.pubmedcentral.nih.gov/articlerender.fcgi?artid=3303607&tool=pmcentrez&rendertype=abstract>  
460
- 461 Pédelacq J-D, Cabantous S, Tran T, Terwilliger TC, Waldo GS. 2006. Engineering and characterization  
462 of a superfolder green fluorescent protein. *Nat. Biotechnol.* [Internet] 24:79–88. Available from:  
463 <http://www.ncbi.nlm.nih.gov/pubmed/16369541>
- 464 Pothoulakis G, Ceroni F, Reeve B, Ellis T. 2014. The spinach RNA aptamer as a characterization tool  
465 for synthetic biology. *ACS Synth. Biol.* [Internet] 3:182–187. Available from:  
466 <http://www.ncbi.nlm.nih.gov/pubmed/23991760>
- 467 Raj A, van Oudenaarden A. 2009. Single-Molecule Approaches to Stochastic Gene Expression. *Annu*  
468 *Rev Biophys*:255–270.
- 469 Rayssiguier C, Thaler DS, Radman M. 1989. The barrier to recombination between *Escherichia coli*  
470 and *Salmonella typhimurium* is disrupted in mismatch-repair mutants. *Nature* 342:396–401.
- 471 Rugbjerg P, Myling-Petersen N, Sommer M. 2015. Flexible metabolic pathway construction using  
472 modular and divisible selection gene regulators. *Metab. Eng.*:in press. Available from:  
473 <http://www.sciencedirect.com/science/article/pii/S1096717615001019>
- 474 Rugbjerg P, Naesby M, Mortensen UH, Frandsen RJ. 2013. Reconstruction of the biosynthetic pathway  
475 for the core fungal polyketide scaffold rubrofusarin in *Saccharomyces cerevisiae*. *Microb. Cell*  
476 *Fact.* [Internet] 12:31. Available from:  
477 <http://www.pubmedcentral.nih.gov/articlerender.fcgi?artid=3654996&tool=pmcentrez&rendertype=abstract>  
478
- 479 Scholz O, Thiel A, Hillen W, Niederwieser M. 2000. Quantitative analysis of gene expression with an  
480 improved green fluorescent protein. *Eur. J. Biochem.* [Internet] 267:1565–1570. Available from:  
481 <http://onlinelibrary.wiley.com/doi/10.1046/j.1432-1327.2000.01170.x/full>
- 482 Shaner NC, Lambert GG, Chammas A, Ni Y, Cranfill PJ, Baird M a, Sell BR, Allen JR, Day RN,  
483 Israelsson M, et al. 2013. A bright monomeric green fluorescent protein derived from  
484 *Branchiostoma lanceolatum*. *Nat. Methods* [Internet] 10:407–409. Available from:  
485 <http://www.pubmedcentral.nih.gov/articlerender.fcgi?artid=3811051&tool=pmcentrez&rendertype=abstract>  
486
- 487 Sievers F, Wilm A, Dineen D, Gibson TJ, Karplus K, Li W, Lopez R, McWilliam H, Remmert M,  
488 Söding J, et al. 2011. Fast, scalable generation of high-quality protein multiple sequence  
489 alignments using Clustal Omega. *Mol. Syst. Biol.* [Internet] 7:539. Available from:  
490 <http://www.pubmedcentral.nih.gov/articlerender.fcgi?artid=3261699&tool=pmcentrez&rendertype=abstract>  
491

- 492 Snapp EL. 2009. Fluorescent proteins: a cell biologist's user guide. Trends Cell Biol. [Internet]  
493 19:649–655. Available from:  
494 <http://www.pubmedcentral.nih.gov/articlerender.fcgi?artid=2784028&tool=pmcentrez&rendertype=abstract>  
495
- 496 Vidal M, Brachmann RK, Fattaey a, Harlow E, Boeke JD. 1996. Reverse two-hybrid and one-hybrid  
497 systems to detect dissociation of protein-protein and DNA-protein interactions. Proc. Natl. Acad.  
498 Sci. U. S. A. [Internet] 93:10315–10320. Available from:  
499 <http://www.pubmedcentral.nih.gov/articlerender.fcgi?artid=38381&tool=pmcentrez&rendertype=abstract>  
500
- 501 Xie XS, Choi PJ, Li G-W, Lee NK, Lia G. 2008. Single-molecule approach to molecular biology in  
502 living bacterial cells. Annu. Rev. Biophys. [Internet] 37:417–444. Available from:  
503 <http://www.ncbi.nlm.nih.gov/pubmed/18573089>
- 504 Yu J, Xiao J, Ren X, Lao K, Xie X. 2006. Probing Gene Expression in Live Cells, One Protein  
505 Molecule at a Time. Science (80-. ). [Internet] 311:1600–1603. Available from:  
506 <http://www.sciencemag.org/content/311/5767/1600.short>
- 507 Zenklusen D, Larson DR, Singer RH. 2008. Single-RNA counting reveals alternative modes of gene  
508 expression in yeast. Nat. Struct. Mol. Biol. 15:1263–1271.
- 509
- 510

510

511 **Table 1** Plasmids employed in this study, describing whether they lead to512 chromosomal integration or propagate autonomously in *S. cerevisiae*.

Plasmid	Expression cassette (promoter-ORF-terminator)	Maintenance in <i>S. cerevisiae</i> through	Reference
pPR4-3vGFP	pSPAL10-3vGFP-tURA3	<i>CEN/ARS, HIS3</i>	This study
pPR4-sfGFP	pSPAL10-sfGFP-tURA3	<i>CEN/ARS, HIS3</i>	This study
pCU2-3vGFP	pCUP1dim -3vGFP-tURA3	<i>CEN/ARS, URA3</i>	This study
pCU3-3vGFP	pCUP1-3vGFP-tURA3	<i>CEN/ARS, URA3</i>	This study
pCfB258-CUP1-3vGFP	pCUP1-3vGFP-tCYC1	Chromosomal integration	This study
pCfB258-CUP1-SPO13-3vGFP	pCUP1dim -3vGFP-tCYC1	Chromosomal integration	This study
pDS1U-X2-3vGFP	pTEF1-3vGFP	Chromosomal integration	This study
pEXP22	pADH1-GAL4AD-RalGDS-tADH1	<i>TRP1</i>	Life Technologies
pEXP32	pADH1-GAL4DBD-Krev1-tADH1	<i>LEU2</i>	Life Technologies
pRS413	-	<i>LEU2</i>	(Sikorski and Hieter, 1989)
pRS415	-	<i>HIS3</i>	(Sikorski and Hieter, 1989)

513

514

515

515 **Table 2** *S. cerevisiae* strains analyzed in this study, indicating which plasmids or

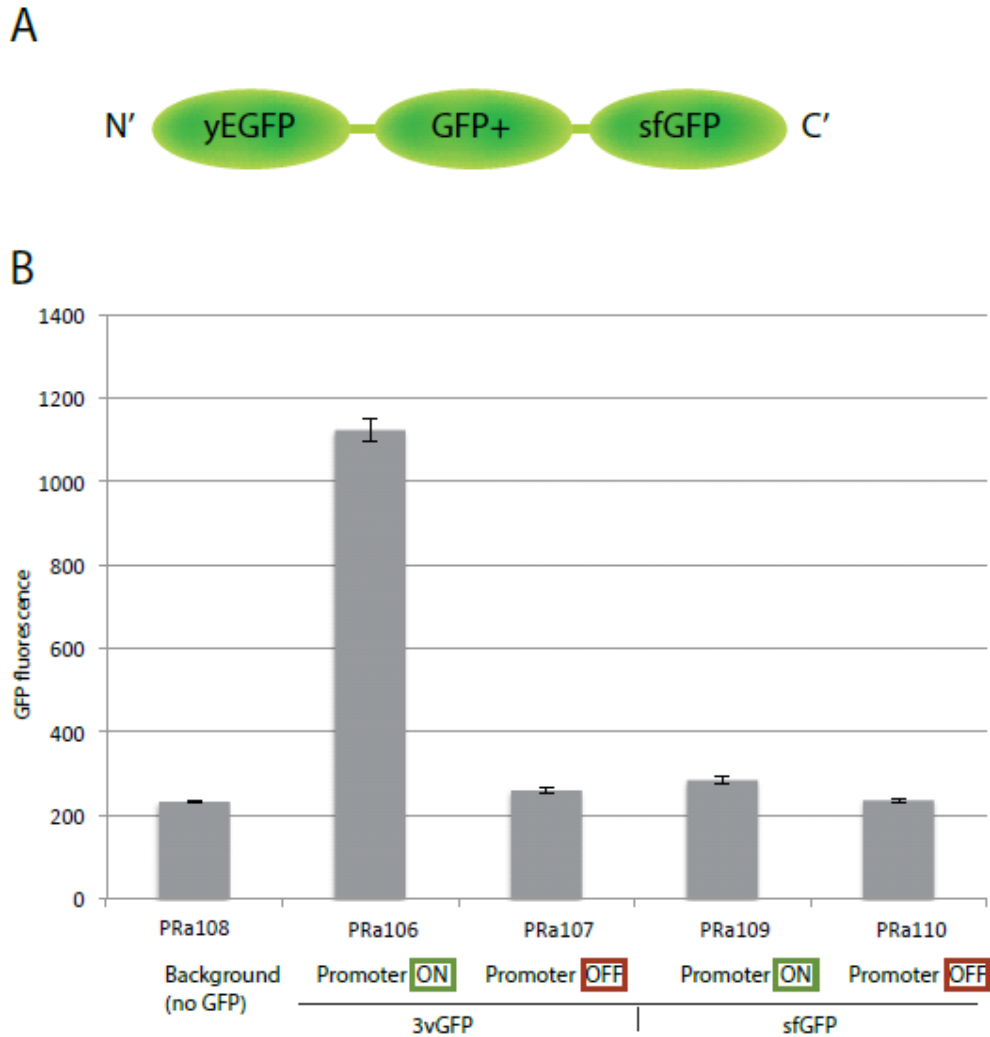
Strain name	Promoter	GFP	Plasmid #1	Plasmid #2	Plasmid #3	Integrative plasmid	Parent strain
PRa106	ON	3vGFP	pPR4-3vGFP	pEXP32	pEXP22	-	PRa26
PRa107	OFF	3vGFP	pPR4-3vGFP	pRS415	pEXP22	-	PRa26
PRa108	-	-	pRS413	pRS415	pEXP22	-	PRa26
PRa109	ON	sfGFP	pPR4-sfGFP	pEXP32	pEXP22	-	PRa26
PRa110	OFF	sfGFP	pPR4-sfGFP	pRS415	pEXP22	-	PRa26
CK24	pCUP1	3vGFP	-	-	-	pCfB258-CUP1-3vGFP	CfB1010
CK28	pCUP1dim	3vGFP	-	-	-	pCfB258-CUP1-SPO13-3vGFP	CfB1010
PRa114	pTEF1	3vGFP	-	-	-	pDS1U-X2-3vGFP	PRa18

516 chromosomal integrations were introduced into the respective parental strains.

517

518

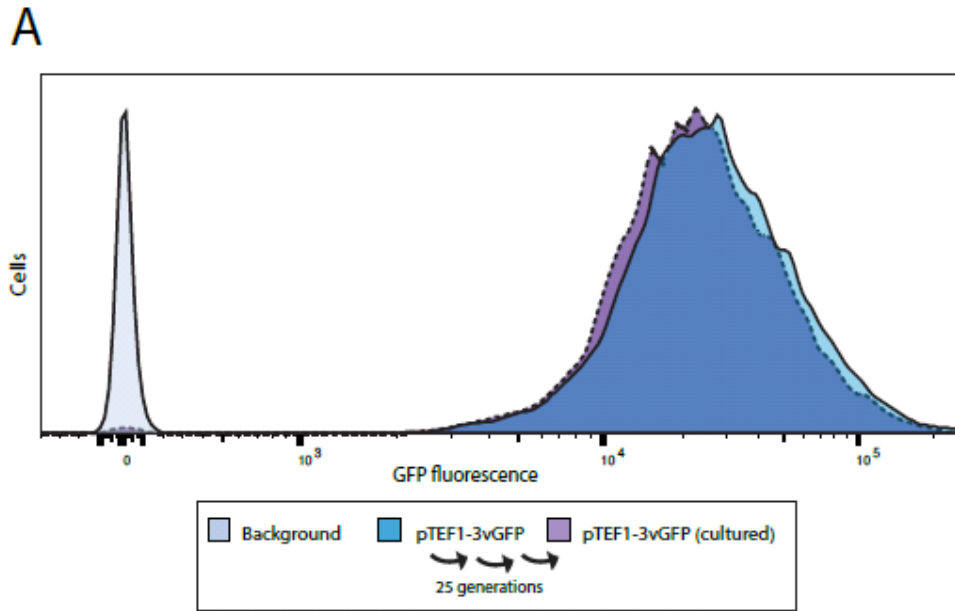




518

519 **Figure 1 Increased GFP fluorescence signal above autofluorescence level by**  
 520 **triple tandem GFP (3vGFP).** A) Internal organization of individual GFP molecules  
 521 fused as 3vGFP. 3vGFP consists of yeast-enhanced GFP (yEGFP), GFP+ and  
 522 superfolder GFP. B) The *S. cerevisiae* strains carrying 3vGFP allowed the capture of  
 523 the weak, ON/OFF promoter pSPAL10 unlike strains carrying a single sfGFP. The  
 524 ON levels with single sfGFP corresponded to the background level of the empty  
 525 control strain without GFP. The strains are described in detail in Table 2. Error bars  
 526 depict standard error from biological replicates (n = 3).

527



**B**

**Nucleotide-level identity**

1: sfGFP	100.00		
2: yEGFP	74.23	100.00	
3: GFP+	76.33	84.45	100.00

**Protein-level identity**

1: sfGFP	100.00		
2: yEGFP	94.12	100.00	
3: GFP+	94.96	96.64	100.00

527

528 **Figure 2 Stability of the triple tandem GFP (3vGFP) towards loop-out**

529 **recombination.** A) Parallel lineages of a pTEF1-3vGFP *S. cerevisiae* strain was

530 cultured for 25 generations and re-measured to verify stability towards loop-out

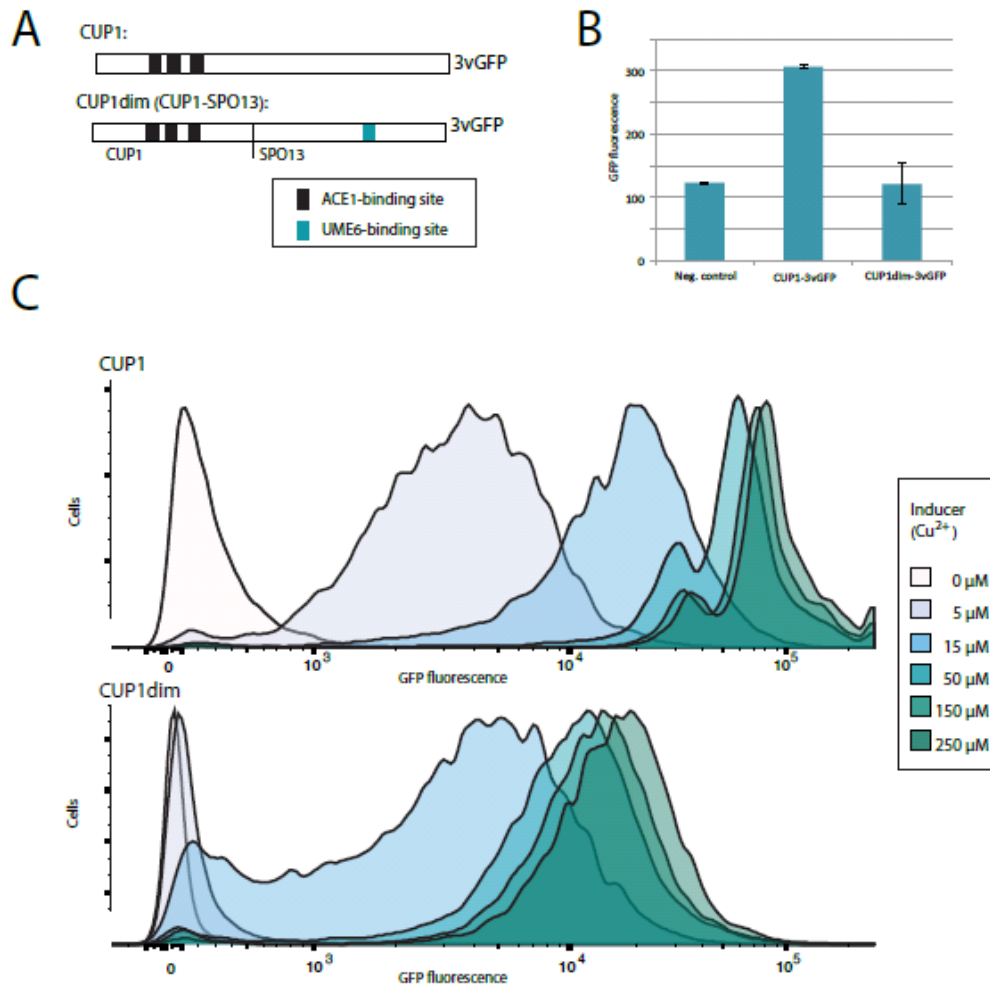
531 recombination, compared to a background strain without GFP. Flow cytometry of

532 representative example shown. Each sample contained 10,000 cells. The maxima of

533 the samples are standardized to an equal top point. B) Sequence identities between the

534 three direct repeats of sequences encoding GFP variants, as calculated by ClustalO.

535



535

536

**Figure 3 Development of weak Cu<sup>2+</sup>-responsive promoter through**

537

**characterization with 3vGFP.** A) Organization of DNA-binding sites for the Cu<sup>2+</sup>-

538

responsive ACE1 activator and UME6 repressor in the wildtype *CUP1* promoter and

539

the new dimmed, hybrid promoter p*CUP1dim*. B) OFF-level fluorescence measured

540

in absence of Cu<sup>2+</sup> demonstrating the lower activity of the new hybrid promoter as

541

captured with 3vGFP. Error bars depict standard error from biological replicates (n =

542

3). C) Fluorescence of strain populations in response to addition of Cu<sup>2+</sup>. Flow

543

cytometry of representative example shown. Each sample contained 10,000 cells. The

544

maxima of the samples are standardized to an equal top point.

545

546

547